

Inverse cascade avalanche model with limit cycle exhibiting period doubling, intermittency, and self-similarity

S. C. Chapman*

Department of Physics, University of Warwick, Coventry CV4 7AL, United Kingdom

(Received 16 November 1999; revised manuscript received 29 February 2000)

A one-dimensional avalanche ‘‘sandpile’’ algorithm is presented for transport in a driven dissipative confinement system. Sand is added at the closed inflow boundary and redistributed when the local gradient exceeds a threshold. The redistribution rule is conservative, nonlocal, and linear and is chosen to mimic fluid flow. Potential energy is dissipated by avalanches that also expel matter at the open outflow boundary. The system then evolves through an inverse cascade. A ‘‘fluidization’’ parameter L_f specifies the length scale over which the algorithm operates. The limiting case of $L_f=1$ cell and $L_f=N$, the system size, are analytically soluble. For other values of L_f the emergent, large-scale dynamics of the system shows a variety of behavior including a limit cycle that has a period-doubling sequence, intermittency, and a random walk.

PACS number(s): 05.45.Ra, 05.10.-a, 45.70.Ht, 05.70.Ln

I. INTRODUCTION

A ubiquitous class of behavior in driven dissipative confinement systems is the absence of intrinsic scales in the statistics and the power spectra of the time evolution of state variables (such as energy) that characterize the dynamics [1]. Currently, distinct theoretical frameworks exist for bursty scale-free energy dissipation; intermittency in a chaotic system caused by a phase space trajectory approaching the critical region of a tangent bifurcation [2] and avalanche (‘‘sandpile’’) models that may in addition exhibit self-organized criticality [3–5]. The former corresponds to a range of values of a control parameter in the underlying dynamical equations for the system; for other values the phase space trajectory may follow a limit cycle. In the latter case, the underlying equations are not known, instead, simple algorithms that prescribe fuelling, redistribution, and thresholds (e.g., a critical value of the local gradient of sand that triggers redistribution only when it is exceeded) are postulated. Importantly in contrast to deterministic chaos these systems are robust: the dynamics is bursty (that is, apparently intermittent) and has scale-free statistics for a broad range of threshold and redistribution algorithms [5].

Coupled map lattices (CML) provide an intermediate class of dynamical system in that continuous equations are first decomposed into a discrete map that is then applied site by site across a grid. For systems of interest the map is nonlinear and local and leads to dynamics across the grid that are self-organizing, and can show the full range of phenomenology associated with chaos (for a review, see [6]). Unlike the avalanche model to be discussed here, CML do not generally include critical thresholds.

Here we present a simple sandpile algorithm that is a generalization of the original Bak, Tang, and Wiesenfeld (BTW) algorithm [3]. In the BTW algorithm, redistribution is ‘‘local,’’ involving nearest-neighbor sites; here we examine redistribution that moves sand over an extended ‘‘fluidization’’ region. The edge-driven model essentially evolves

via an inverse cascade from short to long spatial scales. The redistribution rule is nonlocal and linear so that the large-scale dynamics is a consequence of the interaction of many sites across the sandpile and occurs over many avalanches. This dynamics over the long scales exhibits a range of behaviors reminiscent of deterministic dissipative chaos; but crucially is the emergent phenomenology of a driven dissipative system that is thresholded and as a consequence releases energy by means of avalanches. The model hence provides an important link between the framework of dissipative chaos and self-organization in ‘‘sandpile’’ models.

The model also has physical motivation. Avalanche models with local redistribution rules of which the BTW algorithm is an example, have been associated with diffusion driven transport in astrophysical plasmas (see [7,8] and references therein). We wish to allow the possibility of convective transport in addition to that resulting from thresholded diffusion. A simplified physical example of such a system may be provided by the dynamics of waterdrops on a tilted pane of glass. The fluid forms drops that are at rest until surface tension is exceeded at the leading edge of a drop; drops then reconfigure by fluid flow rather than diffusion alone. The algorithm discussed here then introduces a ‘‘fluidization region’’ such that exceeding the critical threshold prompts redistribution over a region of the sandpile rather than locally. This approach has already had success with plasma confinement systems [9], in particular with the earth’s magnetosphere [10,11] where both diffusion and convection-dominated transport are expected to occur.

II. ALGORITHM

The sandpile is represented by a one-dimensional grid of N equally spaced cells one unit apart, each with sand at height h_j , and local gradients $h_j - h_{j\pm 1}$. A repose gradient z_R is specified below which the sandpile is always stable (the heights h_j and the local gradients are measured relative to this). A critical gradient z_c is also specified and if the local gradient exceeds z_c the sand is redistributed to neighboring cells and iteration produces an avalanche. The critical gradient z_c can be single valued or drawn randomly from a dis-

*Electronic address: sandrac@astro.warwick.ac.uk

tribution; both cases will be considered here. The magnitudes of $\langle z_c \rangle$ and z_R simply scale the total amount of sand and energy in the system.

Sand is added to this edge-driven sandpile at the closed boundary cell 1 at a constant rate $g=1$ (to which we have normalized the h_j and time). The inflow rate is slow compared to the interavalanche time, i.e., $z_c/g \gg 1$ and the dynamics is found to be insensitive to g provided that this condition holds; here we will show results for $\langle z_c \rangle/g = 100$. As soon as the critical gradient is exceeded, the sand is redistributed. The redistribution rule is conservative and instantaneous: avalanches are evolved until at all cells the local gradient is below the critical gradient and only then is further sand added. At each iteration within an ongoing avalanche the height of sand behind the unstable site is reduced so as to flatten a fluidized region $L \leq L_f$ back to the angle of repose; this sand is relocated to the next cell. The flowing region includes all sites behind the unstable site up to either the sandpile boundary or to maximum value L_f , whichever is smaller; L_f is then the fixed control parameter for a given sandpile model of length N . The edge of an ongoing avalanche then propagates forwards from one cell (k) to the next ($k+1$) if

$$h_k - h_{k+1} > z_c. \quad (2.1)$$

This results in a quantity of sand Δ being deposited on the next cell (where * indicates intermediate steps in the relaxation):

$$h_{k+1}^* = h_{k+1} + \Delta \quad (2.2)$$

such that the gradient at cells $k-i$, $i=0, L-1$ relaxes to the angle of repose (here normalized to zero),

$$h_{k-i}^* - h_{k+1-i}^* = z_R = 0, \quad i=0, L-1 \quad (2.3)$$

by conservatively removing sand,

$$h_{k-i}^* = h_{k-i} - \frac{\Delta}{L}, \quad i=0, L-1. \quad (2.4)$$

Equations (2.2)–(2.4) uniquely specify Δ . Here we consider an edge-driven sandpile so that avalanches are forward propagating (i.e., with increasing k). Random or central fuelling could also drive backwards propagation of the avalanche edge (from k to $k-1$) which would then occur if $h_k - h_{k-1} > z_c$ and would be achieved by the same redistribution rule, that is, by adding sand Δ to cell $k-1$ that has been removed conservatively from cells $k+i$, $i=0, L-1$.

An avalanche may be entirely an internal rearrangement of sand or may continue until it spreads across all N cells of the pile (a systemwide discharge) in which case we apply open boundary conditions $h_N^* = h_N = 0$. A state variable of the system is the total potential energy $\epsilon(t_j) = \sum_{k=1}^N h_k^2(t_j)$. The total energy dissipated by an avalanche (internal or systemwide) $d\epsilon$ is then just the difference in the potential energy in the entire sandpile before and after an avalanche.

A major feature of this relaxation rule is that it enforces a minimum length scale L_f for propagation of information (correlation). The model combines the dynamics of avalanching through the inclusion of a critical gradient with a

flowing region where importantly, sand is redistributed although the local gradient is less than critical.

The boundary conditions effectively drive the system at short spatial scales and remove fluctuations at the largest spatial scales; instability (triggering of a new avalanche) will always first occur at cell 1 and then can extend over a region of between 1 and N cells in length, whereas only avalanches of the length N of the system will interact with the outflow boundary.

III. BEHAVIOR OF THE SYSTEM

The system with single valued z_c has two well-understood limiting cases. In the limiting case $L_f=1$ the behavior is just that of the traditional BTW [3] sandpile edge driven in one dimension; in this case the sandpile reaches a unique equilibrium configuration in which the gradients at all cells are just at critical. All avalanches are N cells in length and consist of each added ‘‘grain’’ of sand propagating from the top to the bottom of the pile. In the other limit, $L_f=N$, the behavior is solvable analytically [12]. In this case, an initially empty sandpile can be shown to fill by establishing a height profile that is composed of ‘‘slabs’’ at the repose angle. This arises since (i) the redistribution rule $L_f=N$ ‘‘flattens’’ the region within an avalanche back to the angle of repose and (ii) the start of an avalanche (the first cell to become unstable) in the edge-driven sandpile will always be cell 1 so that avalanches of length L create ‘‘flat’’ regions of sand, i.e., with all cells between 1 and L at the repose angle. An avalanche that is smaller than the preceding avalanche will therefore encounter a flat region of sand in the same way as an avalanche that expands into unoccupied sites; resulting in self-similar dynamics while the sandpile is growing. Once the sandpile encounters the outflow boundary, the entire sandpile empties (i.e., is flattened to the repose angle) and the filling cycle repeats. The time series for energy release is exactly periodic and, on time scales shorter than the period, self-similar. The avalanches are self similar with lengths 2^j , $j=0,1,\dots$, up to the system size, and their statistics for lengths and energy dissipation are inverse power law.

We now first consider all other $1 < L_f < N$ for the simplest case, that is, single valued z_c . In this case we may expect for the edge-driven sandpile that, within a distance L_f of the inflow boundary, the evolution will essentially proceed in a manner similar to the analytic $L_f=N$ system discussed above. This permits the possibility of different dynamics depending on whether L_f is small or of order the system size.

A sandpile in a box of length $N=4096=2^{12}$ has been evolved for each of the redistribution rules $L_f=1,N$. In all cases the system evolves to a state that is not in equilibrium but is such that the energy $E(t)$ has bounded fluctuations about a mean; this state is independent of the initial condition of the sandpile. The lengths of the avalanches that occur in this ‘‘steady’’ state of the sandpile are shown in Fig. 1 for all 4096 runs. This plot provides a phase space portrait of the entire parameter space in the sense that the configurations available to a given sandpile are constrained by the number of different length avalanches that can occur for a given L_f and N . The system is scaling in that a similar plot for a system of length $N=512$ has the same appearance, coarse grained; this is shown in Fig. 2. From the similarity of these

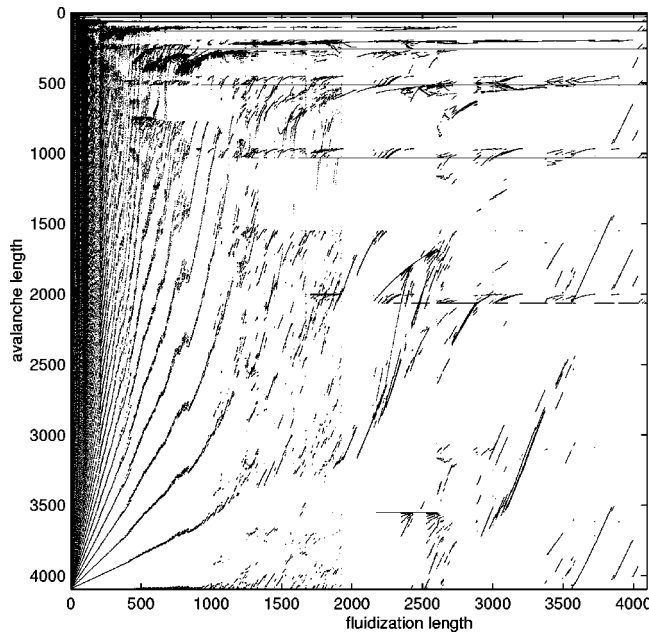


FIG. 1. Lengths of avalanches (abscissa) occurring in the steady state of the sandpile of length 4096 run for all values of the fluidization length L_f (ordinate). The critical gradient is single valued.

plots we expect the control parameter for the dynamics to be L_f/N , and we shall see that the exceptions to this are $L_f = 1, 2$.

In constructing Figs. 1 and 2 sample time series for different values of L_f were first examined to determine the time after which the quasisteady state (with constant mean) had been reached; this time varies with L_f . In order to ensure that the L_f versus avalanche length phase space has been adequately explored, the interval of the time series for each value of L_f spanned $> 10^7 - 10^8$ avalanches.

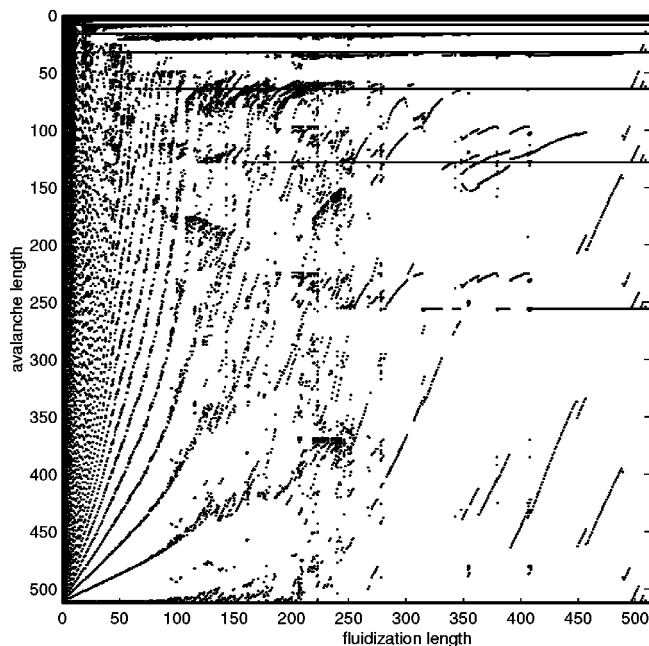


FIG. 2. Lengths of avalanches (abscissa) occurring in the steady state of the sandpile of length 512 run for all values of the fluidization length L_f (ordinate). The critical gradient is single valued.

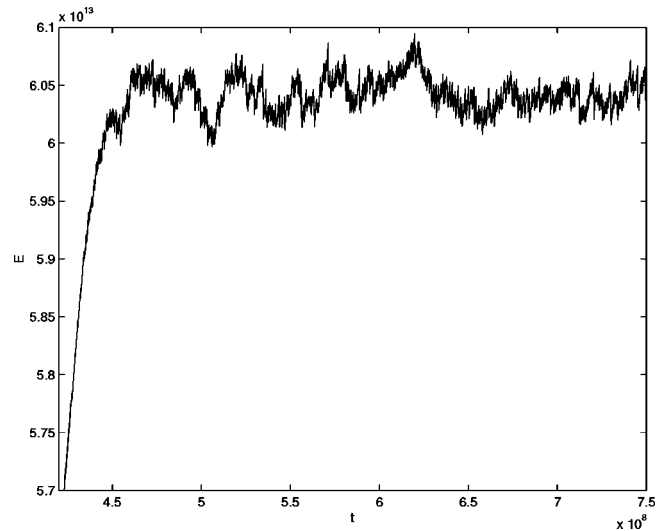


FIG. 3. Time series $E(t)$ of the sandpile with single valued critical gradient of length 4096 run with $L_f=2$ approaching steady state from the initial condition of an empty sandpile.

In the BTW $L_f=1$ limit all avalanches are of length N and appear as a single dot in the bottom left corner of Figs. 1 and 2. This forms a singular point for the intersection of the curves that appear for the cases $L_f < N/4$ approximately. On the right-hand side (rhs) of the plots the $L_f=N$ limit has avalanches of lengths 2^j ; traces of these stretch across the plot as the family of horizontal lines. As we consider sandpiles with smaller L_f , these avalanches of length 2^j are no longer present for successively smaller j . Considerable complexity is evident in the plot and is indicative of a range of dynamical behaviors.

The immediate vicinity of this singular point, $L_f=2$, has a time series that follows a quasirandom walk as shown in Fig. 3. Here we show the system reaching its quasi-steady-state from an initial condition of zero sand in the sandpile. As we increase L_f beyond 2 the dynamics becomes regular. Figures 4–6 show time series for values of $L_f=50, 1024,$ and 2000. These time series show a transition from quasi-

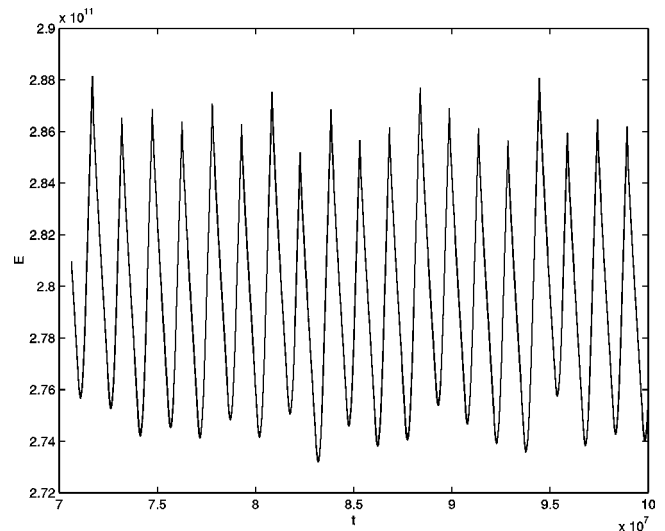


FIG. 4. Time series $E(t)$ of the sandpile with single valued critical gradient of length 4096 run with $L_f=50$ at steady state.

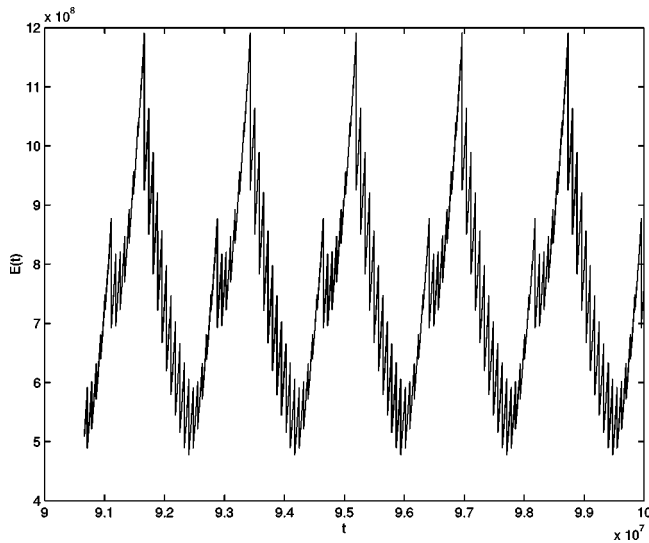


FIG. 5. Time series $E(t)$ of the sandpile with single valued critical gradient of length 4096 run with $L_f=1024$ at steady state.

periodic oscillation ($L_f=50$) through a period doubling ($L_f=1024$) to sawtooth ($L_f=2000$). The latter $L_f=2000 \sim N$ time series is reminiscent of the analytic [12] $L_f=N$ results in that it is, except on scales of order the system size, composed of self-similar avalanches.

We anticipate that this oscillatory behavior has a corresponding limit cycle, and this can be obtained by phase space reconstruction: plotting the energy change in an avalanche dE versus energy E since dE is equivalent to a time derivative here as all avalanches are equally spaced in time. This is shown in Fig. 7 for the $L_f=50$ case. The limit cycle corresponds on the large scale to a roughly parabolic geometry and on the small scale to discrete values of dE on the dE versus E plot. A dE versus E plot for the analytically soluble $L_f=N$ case would be just comprised of lines of discrete values of dE corresponding to discrete avalanches of length 2^j . Here, on spatial scales smaller than L_f the algorithm has

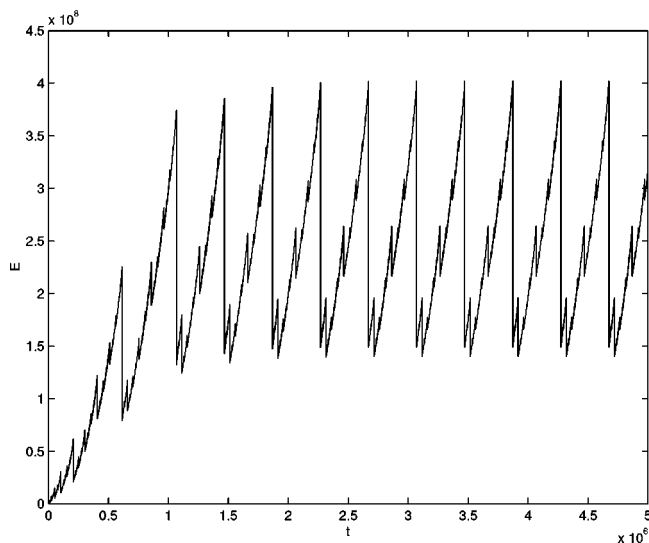


FIG. 6. Time series $E(t)$ of the sandpile with single valued critical gradient of length 4096 run with $L_f=2000$ approaching steady state from the initial condition of an empty sandpile.

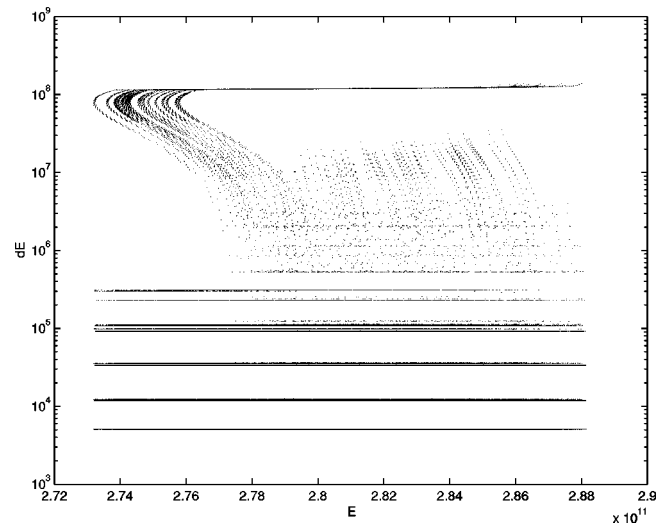


FIG. 7. Phase space portrait dE versus E for the sandpile run with $L_f=50$ at steady state. The dE axis is plotted on a semilogarithmic scale.

approximately the same structure so that on the small scale we can see (on the semilogarithmic plot) equally spaced discrete values of dE that correspond to discrete avalanches of length 2^j that occur on length scales smaller than L_f . This underlying small-scale self-similar structure is found in phase space portraits for all values of L_f and provides the support for the nonrandom nature of the time series. The exceptions, $L_f=1,2$, correspond to the absence of this underlying self-similar structure.

We can now discuss the more physically relevant case where the values of z_c are not identical. The above numerical experiments were repeated with the same mean value of z_c (normalized to the inflow rate g) but with a fluctuation about the mean. Following an avalanche, the value of z_c on each site within the avalanching region is reset before further sand is added. The results are found to be insensitive to both the distribution of the fluctuations on z_c and to its amplitude with respect to the mean; here we show results with a fluctuation amplitude of 1% about the mean which is “top hat” (that is, nonzero and constant in some range $[a,b]$ and zero elsewhere) distributed. A summary of the change in the dynamics with fluctuating z_c is apparent from a plot of the entire parameter space, which is shown in Fig. 8. This has been constructed in the same way as Figs. 1 and 2; here we show the result for a system of length 512 but the basic structure again is found to scale to larger systems. From Fig. 8 we see that the essential structure of the plot is preserved for $L_f/N < 1/4$ approximately, with some broadening of the features seen on Figs. 1 and 2. For larger values of L_f/N the parameter space is radically different, and avalanches of a far wider range of lengths are occurring. The transition in behavior with L_f/N is shown in individual time series taken for the $N=4096$ system; these are shown in Figs. 9–11 for $L_f=50, 1024$, and 2000, respectively. The time series for $L_f/N \ll 1/4$ ($L_f > 2$) essentially have quasiperiodic dynamics that is robust against fluctuations in the normalized critical gradient; the example shown in Fig. 9 has a corresponding limit cycle structure in E, dE space that has the same features as Fig. 7. Once we approach $L_f/N=1/4$ (Fig. 10) the

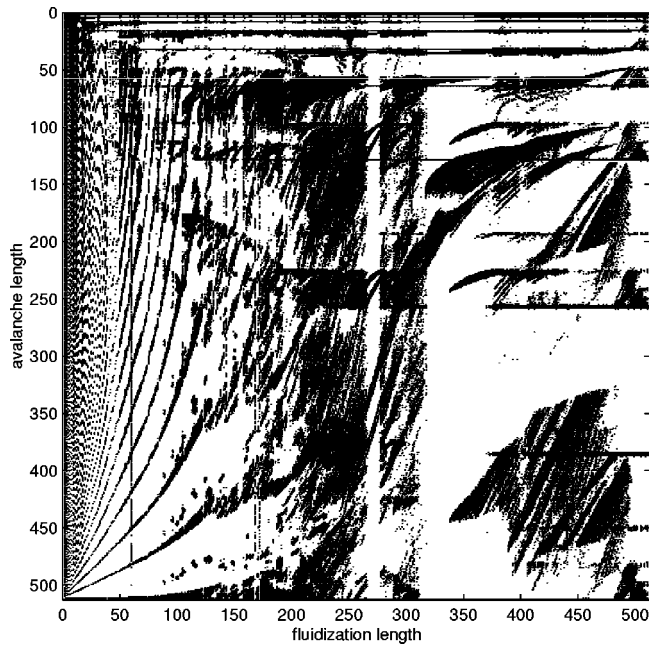


FIG. 8. Lengths of avalanches (abscissa) occurring in the steady state of the sandpile of length 512 run for all values of the fluidization length L_f (ordinate). The critical gradient has 1% fluctuation.

time series become irregular (“intermittent”); time series for larger values of L_f such as $L_f=2000$ (Fig. 11) all show this sensitivity to fluctuations in z_c compared to the single valued case.

An insight into the underlying behavior of these systems is provided by the avalanche statistics. The probability distributions for avalanche lengths and energy dissipated dE have essentially the same morphology for all L_f ; we will therefore focus on avalanche length statistics. Despite the differences in the time series for single valued and fluctuating z_c , the avalanche length distributions shown here are essentially unchanged by adding fluctuations to z_c and we will show examples for the fluctuating case only.

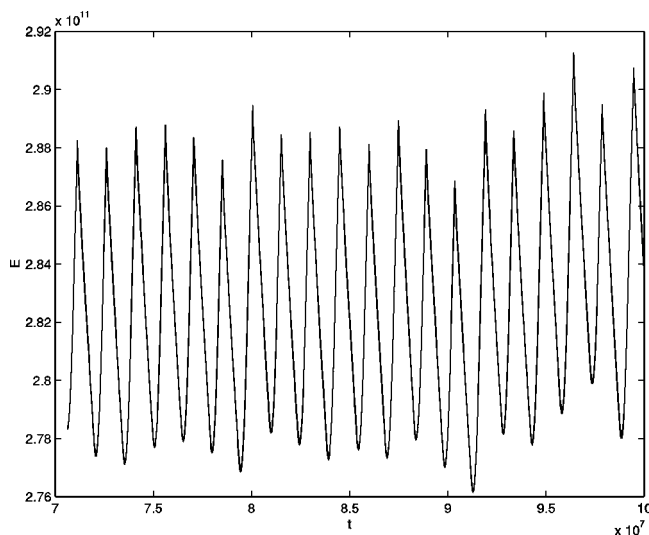


FIG. 9. Time series $E(t)$ of the sandpile with fluctuating critical gradient of length 4096 run with $L_f=50$ approaching steady state from the initial condition of an empty sandpile.

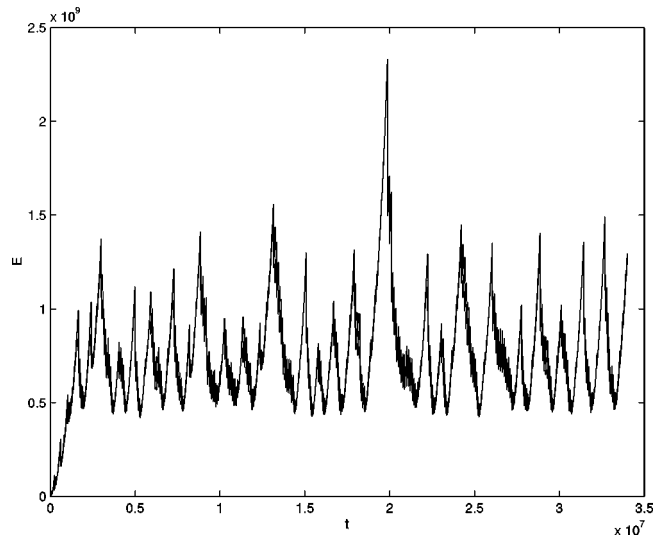


FIG. 10. Time series $E(t)$ of the sandpile with fluctuating critical gradient of length 4096 run with $L_f=1024$ approaching steady state from the initial condition of an empty sandpile.

The probability distributions of avalanche lengths $P(L)$ for $L_f=2, 50, 1024,$ and 2000 (in a system of length 4096) are shown in Figs. 12–15. These show a transition from statistics dominated by a region of approximately power-law slope $+1$ (“random” case $L_f=2$) to statistics with small events of length $<L_f$ that are power law of slope -1 and large events of length $>N-L_f$ of power-law slope $+1$ (quasi- periodic case $L_f=50$) through finally to statistics dominated by power-law slope -1 (irregular cases $L_f=1024, 2000$). This is consistent with the system becoming close to the $L_f=N$ case, which has been shown to possess a fixed point associated with the large avalanches which have power law slope -1 [13].

The small-scale events of length $L < L_f$ occur on or close to $L=2^j$ and have a power-law index -1 and hence suggest dynamics reminiscent of the analytic [12] system. All sys-

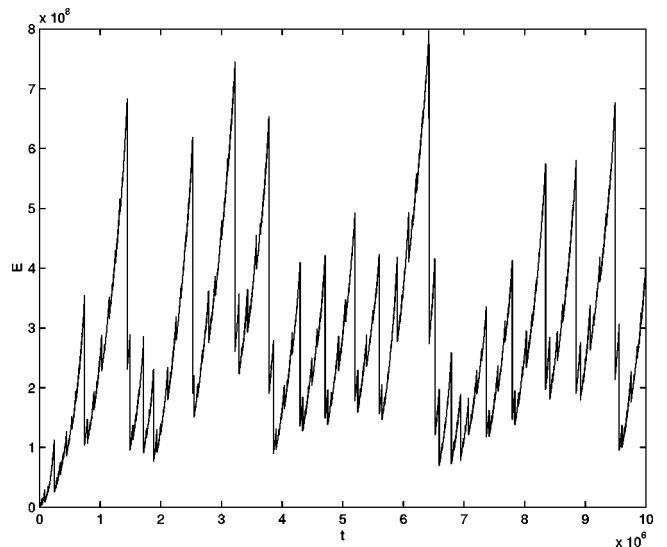


FIG. 11. Time series $E(t)$ of the sandpile with fluctuating critical gradient of length 4096 run with $L_f=2000$ approaching steady state from the initial condition of an empty sandpile.

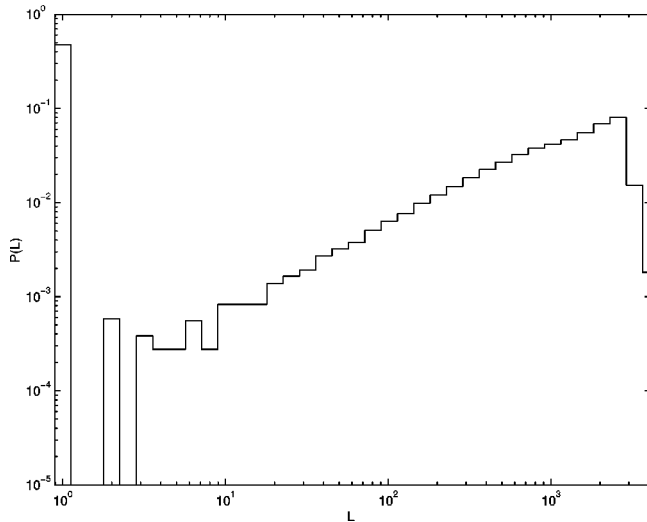


FIG. 12. Probability distribution of avalanche lengths for $L_f = 2$ in a length 4096 sandpile with fluctuating critical gradient.

tems that exhibit limit cycles, such as $L_f = 50$ shown in Fig. 13, are in the range $2 < L_f < N/4$ approximately, i.e., they are examples of systems where L_f and system length N are such as to accommodate avalanches of length $L \ll L_f$ and $N > L > L_f$. Intermittent systems such as $L_f = 2000$ are found in the range $N > L_f > N/4$ approximately and hence avalanches of length $L \gg L_f$ cannot occur; these systems then can only exhibit power-law index -1 events where $L \ll L_f$, which are disrupted around $L \sim L_f$. The “random” system $L_f = 2$ is the only configuration where all structure in avalanches of length $L \sim 2^j$ is disrupted up to $j = 1$, as in this case there is no possibility of $L \ll L_f$. This suggests that the existence of underlying self-similar structure of avalanches on $L \sim 2^j$ is a necessary condition for nonrandom dynamics, and if in addition the system can accommodate avalanches on scales $L \gg L_f$ the characteristic dynamics is limit cycle. It is intriguing to note that this stable limit cycle dynamics corresponds to ($L_f > 2$) systems with the regions within a distance L_f of

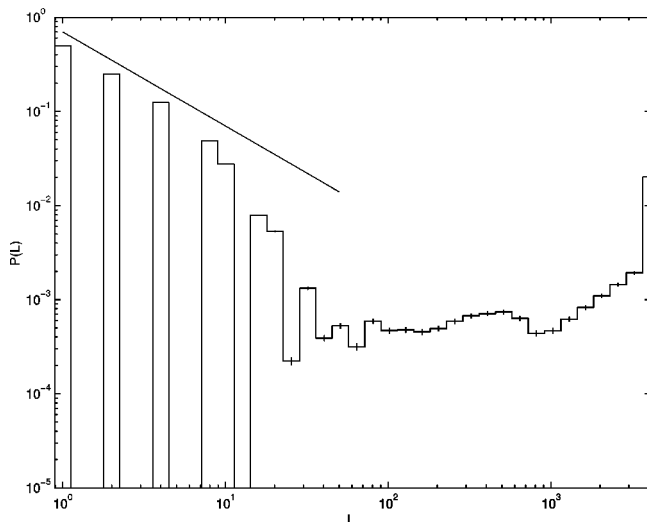


FIG. 13. Probability distribution of avalanche lengths for $L_f = 50$ in a length 4096 sandpile with fluctuating critical gradient. A line $P \sim L^{-1}$ is shown for comparison.

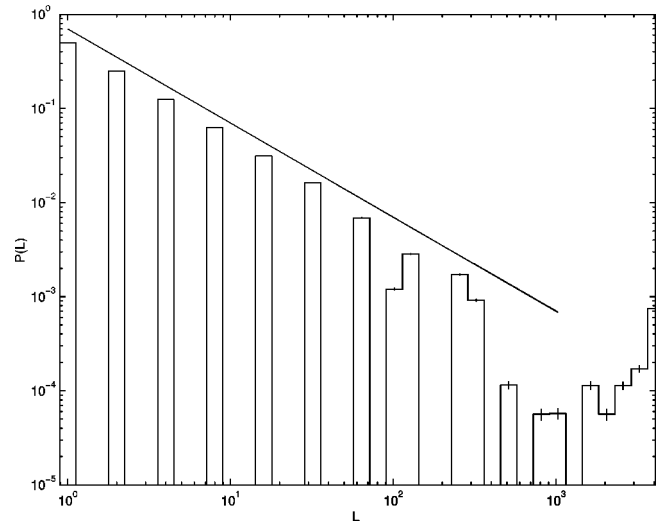


FIG. 14. Probability distribution of avalanche lengths for $L_f = 1024$ in a length 4096 sandpile with fluctuating critical gradient. A line $P \sim L^{-1}$ is shown for comparison.

the boundaries being well separated in the pile. Essentially, the stable regular $2 < L_f < N/4$ systems, and the unstable $L_f \sim N$ systems may correspond to weak and strong coupling of the boundary regions, respectively.

IV. SUMMARY

In conclusion we have generalized the original BTW sandpile algorithm [3] to produce an algorithm for a driven, dissipative system that releases energy by means of (thresholded) avalanches but that exhibits a range of dynamics characteristic of deterministic chaos. The edge-driven system evolves via an inverse cascade from small to large scales, and independent of initial condition evolves to a “steady” state where the total energy fluctuates about some constant mean. The redistribution rule is nonlocal, conservative, and linear, and a single parameter L_f effectively specifies the degree of nonlocality. On the small scale $2 < L \ll L_f$, ava-

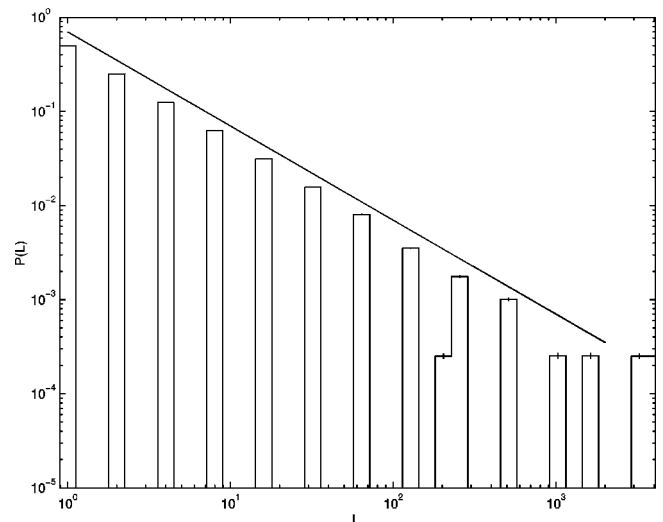


FIG. 15. Probability distribution of avalanche lengths for $L_f = 2000$ in a length 4096 sandpile with fluctuating critical gradient. A line $P \sim L^{-1}$ is shown for comparison.

lanches of length L can have a self-similar structure $L \sim 2^j$ with probability distribution that is power law with index -1 , which may be understood in terms of the analytic limit [12]. On the large scale $L \gg L_f$ the probability distribution is again power law but with index $+1$. If the system length N is such as to accommodate both these $L \ll L_f$ and $L \gg L_f$ regimes (with $L_f > 2$) then the large-scale dynamics follows a limit cycle that is robust against fluctuations in the critical gradient. For larger L_f/N systems, $L \gg L_f$ avalanches cannot occur and the large-scale dynamics is no longer robust against fluctuations in the critical gradient; fluctuations at the 1% level are sufficient to give irregular (“intermittent”) dynamics. The corresponding self-similar scaling in an inverse cascade model may be of significance to turbulent physical systems and will be explored in future work. The cases $L_f = 1$ and 2 do not permit the supporting structure of self-similar avalanches and are equilibrium (see [3]) and a quasi-random-walk, respectively.

In this model the emergent large-scale dynamics is a consequence of the interaction of many sites across the sandpile and occurs over many avalanches. This dynamics over the long scales exhibits a range of behaviors reminiscent of dissipative chaos; but crucially is the phenomenology of a driven dissipative system that is thresholded and as a consequence releases energy by means of avalanches. This may provide insight into a large class of driven dissipative confinement systems, which exhibit self-similarity, emergent and robust global behavior reminiscent of chaotic systems, but on the microscale evolve via avalanches as a consequence of thresholds for transport and energy release.

ACKNOWLEDGMENTS

The author would like to thank G. Rowlands and B. Hnat for illuminating discussions. S.C.C. was supported by the PPARC.

-
- [1] P. Bak, *How Nature Works: The Science of Self Organised Criticality* (Oxford University Press, Oxford, 1997).
 - [2] A. J. Lichtenberg and M. A. Lieberman, *Regular and Chaotic Dynamics*, 2nd ed. (Springer Verlag, Berlin, 1992).
 - [3] P. Bak, C. Tang, and K. Wiesenfeld, *Phys. Rev. Lett.* **59**, 381 (1987).
 - [4] L.P. Kadanoff, S.R. Nagel, L. Wu, and S. Zhou, *Phys. Rev. A* **39**, 6524 (1989).
 - [5] H. J. Jensen, *Self-Organised Criticality: Emergent Complex Behaviour in Physical and Biological Systems* (Cambridge University Press, Cambridge, 1998).
 - [6] *Theory and Applications of Coupled Map Lattices*, edited by K. Kaneko (Wiley, New York, 1993).
 - [7] E.T. Lu, *Phys. Rev. Lett.* **74**, 2511 (1995).
 - [8] D. Vassiliadis, A. Anastasiadis, M. Georgoulis, and L. Vlahos, *Astrophys. J. Lett.* **L53**, 509 (1998).
 - [9] S.C. Chapman, R.O. Dendy, and G. Rowlands, *Phys. Plasmas* **6**, 4169 (1999).
 - [10] S.C. Chapman, N.W. Watkins, R.O. Dendy, P. Helander, and G. Rowlands, *Geophys. Res. Lett.* **25**, 2397 (1998).
 - [11] A. T. Y. Lui, S. C. Chapman, K. Liou, P. T. Newell, C.-I. Meng, M. J. Brittnacher, and G. K. Parks, *Geophys. Res. Lett.* **27**, 911 (2000).
 - [12] P. Helander, S.C. Chapman, R.O. Dendy, G. Rowlands, and N.W. Watkins, *Phys. Rev. E* **59**, 6356 (1999).
 - [13] S. Tam, T. S. Chang, S. C. Chapman, and N. W. Watkins, *Geophys. Res. Lett.* **27**, 1367 (2000).